Cell Lineage Analysis of a Mouse Tumor

Dan Frumkin,[1] Adam Wasserstrom,[1] Shalev Itzkovitz,[2] Tomer Stern,[2] Alon Harmelin,[3] Raya Eilam,[3] Gideon Rechavi,[4] and Ehud Shapiro[1,2]

Departments of [1]Biological Chemistry, [2]Computer Science and Applied Mathematics, and [3]Veterinary Resources, Weizmann Institute of Science, Rehovot, Israel; and [4]Sheba Cancer Research Center and the Institute of Hematology, The Chaim Sheba Medical Center, Tel Hashomer and the Sackler School of Medicine, Tel Aviv University, Tel Aviv, Israel

Abstract

Revealing the lineage relations among cancer cells can shed light on tumor growth patterns and metastasis formation, yet cell lineages have been difficult to come by in the absence of a suitable method. We previously developed a method for reconstructing cell lineage trees from genomic variability caused by somatic mutations. Here, we apply the method to cancer and reconstruct, for the first time, a lineage tree of neoplastic and adjacent normal cells obtained by laser microdissection from tissue sections of a mouse lymphoma. Analysis of the reconstructed tree reveals that the tumor initiated from a single founder cell, ~5 months before diagnosis, that the tumor grew in a physically coherent manner, and that the average number of cell divisions accumulated in cancerous cells was almost twice than in adjacent normal lung epithelial cells but slightly less than the expected figure for normal B lymphocytes. The cells were also genotyped at the *TP53* locus, and neoplastic cells were found to share a common mutation, which was most likely present in a heterozygous state. Our work shows that the ability to obtain data regarding the physical appearance, precise anatomic position, genotypic profile, and lineage position of single cells may be useful for investigating cancer development, progression, and interaction with the microenvironment. [Cancer Res 2008;68(14):5924–31]

Introduction

Despite several decades of scientific research, basic properties of the growth and spread of tumor cells remain controversial (1). This may seem surprising because cancer is primarily a disturbance of cell growth and survival, and an aberrant growth pattern is perhaps the only property that is shared by all cancers. However, because the initiation and much of the subsequent development of tumors occurs before diagnosis, studying the growth and spread of tumors seems to require retrospective techniques, and these have not been forthcoming.

In the last several years, quantitative analysis of somatic genetic mutations has emerged as a powerful research tool, which is capable, due to its retrospective nature, of obtaining information on the early stages of tumor development.

The approach was pioneered by Shibata and colleagues (2), who suggested that mutations in microsatellite (MS) loci act as "molecular tumor clocks" that record past tumor histories, and showed this concept by uncovering mechanisms underlying colorectal pretumor progression (3–6). A similar approach was also used by a different group in the investigation of breast carcinoma (7). Recently, a team led by Maley and colleagues (8, 9) showed that quantitative analysis of MS mutations could also be used prospectively to predict progression from a precancerous lesion to adenocarcinoma.

We recently showed that quantitative analysis of somatic mutations could be used for reconstructing cell lineages (10). We developed a method based on this principle, showed its precision in an *ex vivo* system (10), and implemented it *in vivo* by reconstructing mouse cell lineage trees (11). Recently, a similar method was independently developed by a different team and also used to investigate cell lineages in a mouse (12, 13). Our team continued advancing the capabilities of the method by incorporating into it a method for estimation of absolute cell depths (number of mitotic divisions since the zygote; ref. 14) and a protocol for performing whole genome amplification (WGA) of single cells obtained from stained tissue sections by laser-assisted microdissection (LAM; ref. 15). We then set out to use the method for studying cancer cell lineages.

The classic model of tumorigenesis was developed in the 1970s (16, 17). According to it, a tumor is derived from a single founder cell that has acquired a growth advantage over normal cells by a genetic modification. The progeny of the founder cell expands in an evolutionary pattern, in which more aggressive cells and their descendants become increasingly predominant in the tumor cell population, eventually giving rise to drug-resistant and metastatic subclones.

Although the model is still widely accepted today (18, 19), several aspects of it, such as the monoclonal origin of tumors and the late onset of metastases from rare tumor cell populations, are increasingly being challenged (20–25).

The validity of the classic model of tumorigenesis could be easily investigated by cell lineage reconstruction because the model implies lineage relationships that should be readily apparent in the topology of a tumor cell lineage tree. Specifically, the tumor cell population should appear as a subtree within the entire organism cell tree, metastases should appear as subtrees within the tumor subtree, and the founder cells of metastatic subtrees should reside at much greater depths than the founder cell of the tumor (Fig. 1). Furthermore, because the topologies of cell lineage trees encode a vast amount of biological information, analysis of tumor trees could also be used to obtain additional information, allowing for development of new models.

Note: Supplementary data for this article are available at Cancer Research Online (http://cancerres.aacrjournals.org/).

E. Shapiro is the Incumbent of The Harry Weinrebe Professorial Chair of Computer Science and Biology and of The France Telecom-Orange Excellence Chair for Interdisciplinary Studies of the Paris "Centre de Recherche Interdisciplinaire."

G. Rechavi holds the Djerassi Chair in Oncology at the Sackler Faculty of Medicine, Tel-Aviv University.

Requests for reprints: Ehud Shapiro, Weizmann Institute of Science, Herzl Street, Rehovot 76100 Israel. Phone: 97289344506; Fax: 97289344484; E-mail: ehud.shapiro@weizmann.ac.il.

doi:10.1158/0008-5472.CAN-07-6216

Here, we reconstruct a cell lineage tree of cancerous and adjacent normal cells extracted from tissue sections of a mouse lymphoma. Analysis of this tree reveals several aspects of the developmental history of the tumor, including its monoclonal origin, the physically coherent growth pattern of the tumor, depth of cancer cells and adjacent normal lung epithelium, the age of the tumor, and the presence of a mutation in the *P53* gene in a heterozygous state.

Materials and Methods

Mouse. Mlh1+/− mice were obtained from Michael Liskay (Oregon Health and Science University, Portland, Oregon; described in ref. 26) and were maintained at our institute under a dual genetic background (C57Bl/6 and 129SvEv). All work was done under the Weizmann Institute of Science Institutional Animal Care and Use Committee approval. The experimental animal was sacrificed by CO_2 asphyxiation. Extracted tissues were either fixed in 10% formaldehyde solution for 24 h or snap frozen in liquid nitrogen, and stored in −80°C until use.

Deparaffinized 3-μm sections were stained with H&E according to standard protocols.

Immunohistochemistry. Staining of mouse tissue sections was performed according to the protocol described by Aharoni and colleagues (27). Antibodies used were rat anti-human CD3 (Serotec; final concentration 1:100) and Hoechst 33342 (Molecular Probes; final concentration 1:2,000).

Tissue section preperation, LAM, and WGA. Preperation of tissue sections, cell isolation, LAM, DNA extraction, and WGA were performed as described by Frumkin and colleagues (15). Briefly, frozen mouse tissues were cut to 6-μm sections, mounted on membrane-coated slides, and stained with H&E. Single cells were microdissected from the sections and catapulted into adhesive caps of 200 μL microtubes. DNA extraction was performed by alkaline lysis directly on the cap surfaces. WGA was performed using the GenomiPhi DNA amplification kit (Amersham Biosciences), with modifications, and aliquots of WGA products were used directly (without purification) as templates in subsequent PCRs. Negative control samples (containing no cells) were created for each tissue section and subjected to the same procedures as the cell samples.

Cell lineage reconstruction. Each single cell was genotyped at 120 MS loci (Supplementary Table S1) using a semiautomated procedure, and a quantitative comparison of the genotypes (i.e., "Cell identifiers"; Supplementary Table S2) yielded a reconstructed tree. This was performed in a similar fashion to that described by Frumkin and colleagues (10). A full description of all procedures is provided in Supplementary Text S1.

Cell depths. For each cell in the reconstructed tree, the sum of the vertical Neighbor-Joining branch lengths leading to it from the tree root was multiplied by 256 (obtained from ref. 14), yielding absolute depth in cell divisions. The probability that depths of cancer and normal cells were from the same distribution was calculated using a Kolmogorov-Smirnov test applied to the cancer and normal cell depth distributions.

Coherent growth. To assess the correlation between physical and lineage distance, we used the sum of branch lengths that connects both cells to their most recent (i.e., deepest) common ancestor as a lineage distance measure. The distribution of lineage distances between pairs at different distances was compared using Student's t tests.

Results

MLH1−/− mice (26), which are known to have a high rate of mutations in MS loci, and to develop a variety of spontaneous tumors (28), were grown under normal conditions. A male mouse

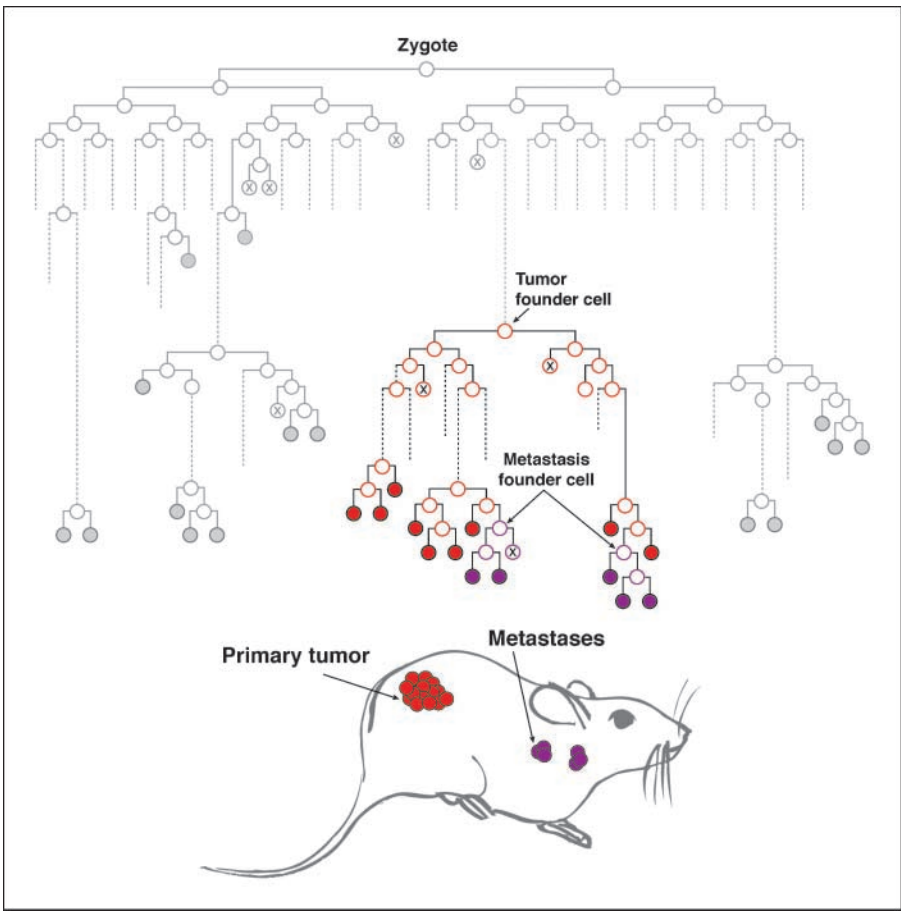

Figure 1. Cancer cell lineage. According to the classic model of tumorigenesis, cancer starts from a single transformed cell that gives rise to all cancer cells, and metastases are formed from single cancer cells that underwent further genetic alterations. The figure depicts a mouse in which a cancer has developed according to the classic model and how this is reflected in the topology of its cell lineage tree. Primary tumor cells (*red*) are clustered in a subtree of the complete organism cell tree, and metastatic cells (*purple*) are clustered on secondary subtrees within the cancerous subtree. Founder cells of metastases reside at a much greater depth (vertical distance from the zygote) than the founder cell of the tumor because according to the model, metastasis formation occurs late in tumorigenesis.

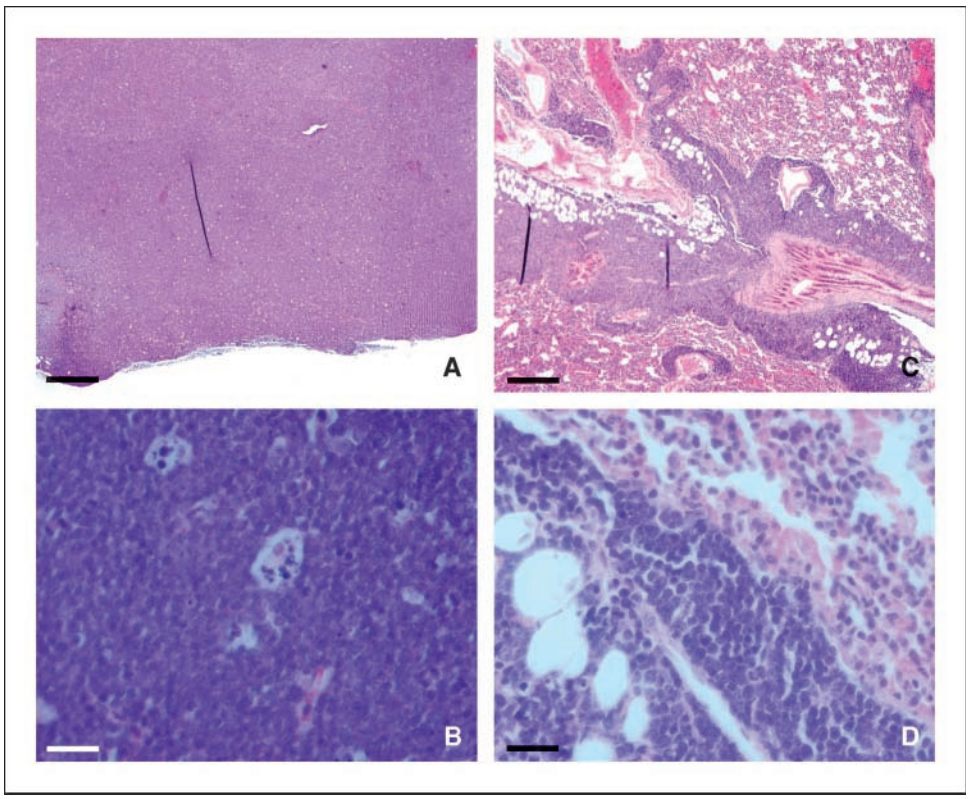

Figure 2. Tumor histology. *A,* mediastinal tumor mass under low magnification. *Bar,* 500 μm. *B,* mediastinal tumor mass under high magnification, showing tingible body macrophages. *Bar,* 25 μm. *C,* left lung showing infiltrate of tumor cells. *Bar,* 500 μm. *D,* high magnification of the left lung, showing the border area between the tumor focus and adjacent normal lung epithelium. *Bar,* 25 μm.

developed dyspnea and general poor appearance at the age of 9 months. The animal was sacrificed and pathologic examination revealed a round white tumor mass (diameter, 9 mm) in the anterior mediastinum and similar foci in the right and left lungs. Tissue samples from all tumor foci were resected, and each sample was cut into two portions—one was snap frozen and the other was fixed in formaldehyde. Examination of stained fixed tissue sections revealed the thoracic tumor mass to consist of irregular, poorly differentiated cells with large nuclei, scant cytoplasm, and central nucleoli, interspersed with tingible body macrophages in a "starry sky" configuration that is typical of lymphomas (Fig. 2*A* and *B*). Examination of the stained lung sections revealed foci consisting of the same type of cells as in the thoracic mass, well-demarcated from the normal lung epithelium (Fig. 2*C* and *D*). Immunohistochemical analysis revealed that tumor cells from all foci expressed the CD3 protein on their cell membranes, indicating that the tumor was a T-cell lymphoma (Fig. 3).

Lineage analysis of single cells from tumor microenvironments requires precise isolation of desired cells and subsequent amplification of the entire genome. To this end, we made use of a protocol that we recently developed for genome amplification of laser-microdissected single cells isolated from stained tissue sections (15). Before isolation, each cell was photographed and classified according to its anatomic location, specific tissue section, and histologic appearance. Cells isolated from tumor foci received a histologic classification of "cancerous," whereas cells isolated from normal lung epithelium were classified as "normal" (Supplementary Table S3).

From each single cell, DNA was extracted, amplified by WGA, and genotyped at 120 MS loci by PCRs and capillary electrophoresis. The success rate of WGA varied between different cells and between different MS loci. On average, ~83 alleles were successfully amplified from each cell, representing 38.5% of the 216 possible alleles. For each cell, the electrophoresis signals of PCR products were compared with corresponding signals from DNA extracted from a tail clipping of the same animal, which represented the DNA of the zygote (for explanation, see Supplementary Text S2). MS slippage mutations (29) were detected as differences in allele lengths between the cell and zygote samples, corresponding to whole basic repeat units (see examples in Supplementary Fig. S1). The end product of this comparison was a "digital identifier" (10) for each cell, representing the mutational status at each amplified locus (Supplementary Table S2). Identifiers were processed by a phylogenetic algorithm implementing the neighbor-joining method (30), yielding a reconstructed cell lineage tree, which was rooted from the zygote sample. By incorporating data from Wasserstrom and colleagues (14), a depth scale bar was created, allowing for translation of vertical branch distances in the tree into absolute numbers of cell divisions. The tree and accompanying depth scale bar are presented in Fig. 4. Analysis of the reconstructed tree revealed several aspects related to the growth of the tumor:

All tumor cells have a common clonal origin. All cells isolated from the three tumor foci are clustered on a single subtree, whereas 11 of the 14 cells isolated from the normal lung epithelium are positioned outside this subtree. This clustering pattern supports a common clonal origin for all tumor cells. To determine whether this result is statistically significant, we used hypergeometric tests to score the observed clustering of cancer cells in the reconstructed tree and then compared this score to scores of reference trees, generated by random permutation of the leaves on the observed topology (Supplementary Text S3). The score of the reconstructed tree is higher than the score of all 10,000 randomly generated trees. Furthermore, a qualitative comparison between physical and

lineage positions of cells reveals that the lineage restriction between the tumor subclone and the rest of the tree coincides closely with the physical border between tumor foci and adjacent normal tissues (example in Fig. 4*D*). The tumor subtree is not exclusive, as three cells isolated from normal epithelium are also positioned in it. However, the labeling and position of these cells in the reconstructed tree are questionable (see Discussion).

In the reconstructed tree, cells from the tumor foci in the right and left lungs do not form exclusive secondary subtrees within the tumor subtree, as would be expected of metastases according to the accepted model of tumorigenesis (compare Fig. 1–Fig. 4*A*). This result, together with the observation that the tumor foci in both lungs were large, occupying significant portions of the lungs and extending to their borders, suggests that the tumor spread from the mediastinum into both lungs by local invasion, rather than by metastasis formation.

Lineage distance among cancer cells is correlated to their physical distance. Cancer cells are not randomly distributed within the tumor subtree but rather tend to cluster together in groups that correspond to the different physical locations that the cells were isolated from. To quantify this clustering pattern, we divided the cells into three categories corresponding to increasing physical distances and calculated the mean lineage distance (see definition in Materials and Methods) within each category and between the different categories. The mean lineage distance was smallest between cells obtained from the same tissue section, larger for cells from different sections within the same tumor focus, and largest for cells from different foci (Fig. 4*B*). All differences in distances were significant, reflecting a significant correlation between physical and lineage distances in the tumor cell population.

Cell depths. The depths of cells in the reconstructed tree ranged from 62 to 300 cell divisions (Fig. 4*A*). The mean depth of cancer cells was 236, whereas the mean depth of normal lung epithelial cells was 121 (Fig. 4*C*). Normal T lymphocytes were not extracted from the animal, and therefore, the depth of tumor cells could not be compared directly to the depth of their normal counterparts. However, an indirect comparison can be made to the expected depth of B-lymphocytes, which were previously shown by our group to divide at an approximate rate of one cell division per day in mice with the same genetic background (14). Based on this information, B lymphocytes in a 9-month-old mouse are expected to be at a depth of ~274 cell divisions, which is slightly deeper than the observed figure for neoplastic T cells in the present study (Fig. 4*C*).

The significant difference in depths between cancer cells and normal lung epithelial cells ($P = 2.1*10^{-5}$; Fig. 4*C*) most likely reflects a difference in the underlying cell turnover rate between the two functionally distinct cell populations (see Discussion).

The tumor is about 5 months old. By assuming that both tumor cells and their normal progenitors divided at the same rate, it is possible to estimate the age of the tumor. The founder cell of the tumor subtree (which represents the founder cell of the final clonal expansion) resides at a depth of 102 cell divisions, 134 cell divisions younger than the average cancer cell. Therefore, considering that the animal was sacrificed at the age of 275 days, the tumor can be estimated to have started growth at the age of ~119 days (102/236*275), and to have proceeded for ~156 days before diagnosis.

Tumor cells share a heterozygous *TP53* mutation not shared by normal cells. We genotyped the *TP53* gene because mutations in this gene are very common in human and mouse cancers and

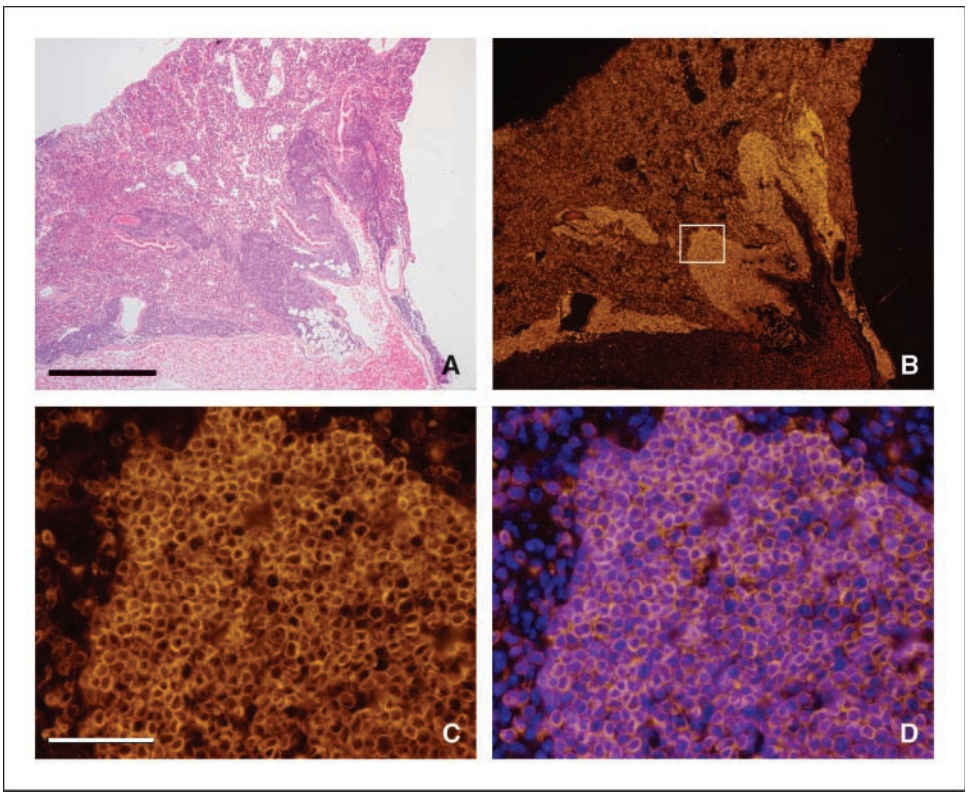

Figure 3. Immunohistochemistry. *A,* a section of the right lung stained with H&E. *Bar,* 500 μm. *B,* a section of the right lung, adjacent to the section shown in *A*, stained with anti-CD3 antibodies. *C,* close-up view of the area in *B* that is delineated by a rectangle, showing the border between the cancerous focus and adjacent normal lung epithelium. *Bar,* 50 μm. *D,* the same area as in *C* with double staining for anti-CD3 and Hoechst nuclear stain. CD3 expression can be seen on the cell membranes of tumor cells. A similar pattern was observed for the mediastinal tumor mass and for the left lung (data not shown).

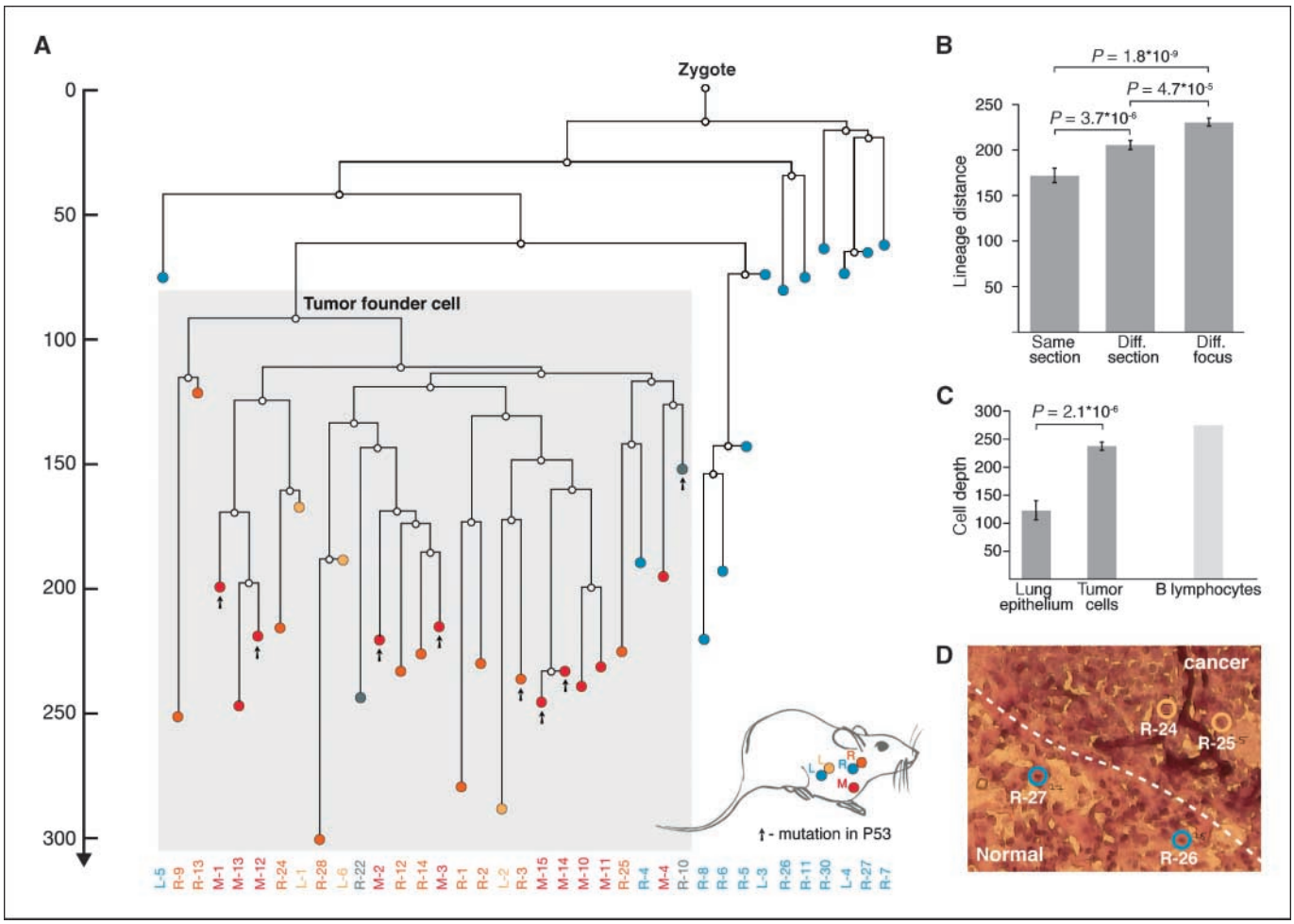

Figure 4. Cancer cell lineage reconstruction. *A,* reconstructed cell lineage tree. All cells from the mediastinal tumor mass (*M*; *red*), and from cancer foci in the right (*R*; *orange*) and left (*L*; *yellow*) lungs are clustered on the same subtree (*highlighted gray*), whereas most cells from the normal epithelium of the right (*R*; *blue*) and left (*L*; *blue*) lungs are clustered outside this subtree. Cells R-10 and R-22, which were positioned on the border region between the tumor focus and adjacent normal tissue in the right lung, are colored gray. Founder cell of the cancer subtree is indicated. The vertical axis on the left represents estimated cell depth (number of cell divisions since the zygote). *B,* correlation between lineage and physical distances. The mean lineage distance between cells from the same tissue section is the smallest, followed by cells from different sections in the same focus, and cells from different foci. *C,* mean depth of cancer cells is almost twice the mean depth of normal lung epithelial cells but slightly less than the expected depth of B lymphocytes in an animal of the same age. *D,* tissue section from the right lung. *Dashed white line,* the border between the cancerous and normal tissue. Cells R-24, R-25, R-26, and R-27 are outlined.

are believed to play an important role in cancer pathogenesis (31). Specifically, we focused on exon 8, which has been reported to contain a "mutational hotspot" in codon 270 (32). We amplified and sequenced a 240 bp fragment, spanning the mutational hotspot and analyzed the sequences. The tail clipping DNA contained no mutations, whereas some of the single cells contained the same specific C→T mutation in codon 270 (Fig. 4*A*). In the subset of cells obtained from tumor foci, 10 cells failed to amplify completely, 5 cells showed only the mutant genotype, 6 showed only the wild-type (wt) genotype, and in 2 cells (M-3 and M-14), both mutant and wt genotypes were detected (Fig. 5). In the subset of cells isolated from normal epithelium, five cells failed to amplify completely, eight showed only the wt phenotype, and cell R-10, which was originally labeled as "normal," but which likely represents a case of "mistaken identity" (see Discussion), was heterozygous for the mutation, displaying both the mutant and wt genotypes. There are several possible explanations for the finding of identical mutations in some, but not all, tumor cells. The mutation may have arisen as multiple independent events or as a single early event. It may be present in all tumor cells but only detectable in some cells due to allele drop out, or conversely, it may be present in only a subset of cells, and in the latter scenario, the subset may be a subclone of the tumor or a nonclonal subset. The wt genotypes may represent nonmutated alleles or alleles that reverted back to the wt state by a second mutation. Of all of the possibilities outlined above, the most likely is that the mutation arose as a single event in the primary tumor cell in one of the alleles was present in all tumor cells in the heterozygote state but was not detected in all cells due to allele drop out. A discussion of the likelihood of all the possibilities and a statistical analysis supporting the most likely possibility are presented in Supplementary Text S4.

Discussion

This work shows a new approach for studying cancer. Analysis of 37 single cancer and adjacent normal cells was sufficient to establish the monoclonal origin of the tumor cells, calculate depth of cancerous cells and normal lung epithelium cells, calculate the

age of the tumor, characterize the growth pattern of the tumor, and to detect the presence of a *TP53* mutation in cancer cells in the heterozygous state. Although general conclusions regarding cancer cannot be drawn from a single case study, we hope that this demonstration of the usefulness of the approach will motivate its future use in cancer research. A discussion of specific results and possible applications is presented below.

Tumor subtree. In the reconstructed tree, all tumor cells are clustered on a single subtree, indicating a monoclonal origin, and this result is in line with the classic model of tumorigenesis. However, the tumor subtree also contains three cells that were initially labeled as "normal" (R-4, R-10, and R-22). Cells R-10 and R-22 were isolated from the tumor-normal epithelium border and were originally considered to be normal as they appeared to reside on the epithelium side of the border. In retrospect, these cells likely represent mistaken identity (i.e., they were actually cancer cells), as the precise border of the tumor was sometimes difficult to determine under the highest magnification. This possibility gains support from the fact that R-10 contained a mutant *TP53* allele, which was also found in seven tumor cells but in no other normal cell. In contrast, cell R-4 was isolated from an area of the lung epithelium not adjacent to any tumor focus. The clustering of R-4 within the tumor subtree raises the possibility that the cell was a descendant of tumor cells, which migrated to an area of normal lung epithelium and underwent "reversion" from a cancerous to a normal phenotype. Although the classic model of tumorigenesis (16, 17) does not explicitly rule out such a possibility, it is generally assumed that cancer progression is a "one way road." In some tumors, however, such as neuroblastoma, spontaneous or therapy-induced differentiation of malignant cells to mature, normal-appearing cells can occur. However, WGA from R-4 has a low yield compared with other cells (28% for R-4 versus a mean of 38.5% for all cells), and therefore, its position in the reconstructed tree may be less reliable than the position of most other cells. The precision of tree reconstruction depends mainly on the "signal to noise" ratio (10), which is higher for cells in which a relatively large number of loci were successfully amplified, and lower for cells with poorer amplification. Thus, the low signal from cell R-4 might have resulted in misplacing of the normal cell within the tumor subtree. We therefore consider it most likely that the results do not support reversion of cancer cells to normal phenotype, and that the tumor cell population in the mouse was indeed an exclusive clone. It is important to note that although the tumor subtree contains cells that are on average much deeper than the rest of the cells in the tree, the algorithm that was used for reconstruction (i.e., neighbor joining using the absolute distance metric) is relatively insensitive to such biases as it iteratively groups pairs of samples that are both close to each other in the specified distance metric and far from all other samples. Specifically, the algorithm does not tend to cluster together cells that are deeper than other cells, as can be evident by the fact that normal cell R-8 is deeper than 11 of the cells in the tumor subtree, yet it is situated outside of the tumor subtree. In general, the algorithm clusters together cells on the basis of their shared developmental path and had there been multiple unrelated tumors in the mouse, all originating at about the same time but

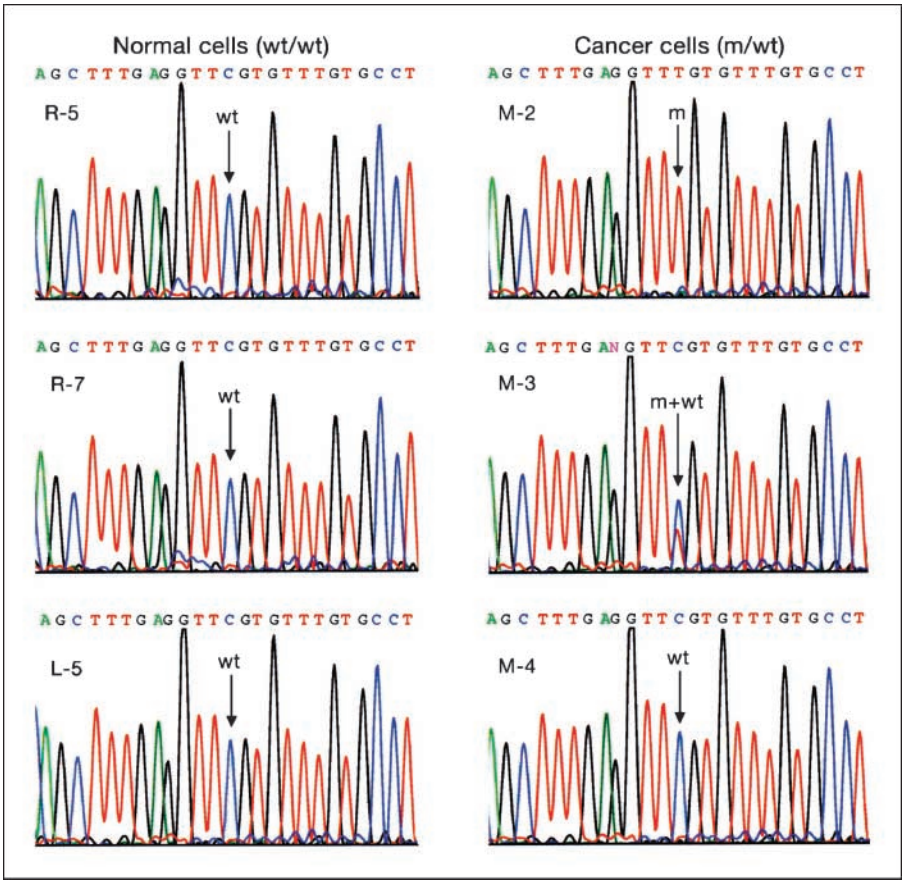

Figure 5. *TP53* sequences. Normal cells show only the wt sequence at codon 270, whereas cancer cells show either the wt sequence, the C→T mutation (*m*), or both wt and mutant sequences together (cell M-3). These results suggest that normal cells are homozygous to the wt allele (*wt/wt*), whereas cancer cells contain one wt and one mutant allele (*m/wt*).

from different founding cells, the algorithm would detect it and output a reconstructed tree with discrete tumor subtrees (corresponding to the different tumors), interspersed with normal cells.

Correlation between physical and lineage distances. The significant correlation between the physical and lineage distances within the tumor cell population is most likely a result of a coherent growth pattern, wherein daughter cells do not tend to migrate but rather remain physically close after cell division (33). Although the results suggest that most cells did not migrate, some migration in a minority of tumor cells cannot be ruled out. The absence in the literature of quantitative empirical data on cell lineage relations within tissues with established growth patterns hinders the possibility of providing a quantitative description of cell migration in the present study. We believe that with time, as *in vivo* cell lineage data accumulates from different experiments, the ability to provide a quantitative description of cell migration patterns will materialize.

Cell depths. The ability to estimate the depth of a cell from the amount of slippage mutations that accumulated in its genomic MS loci stems from the fact that these mutations represent independent events that occur during DNA replication and are therefore coupled to cell divisions (10). We previously showed that in *in vitro* cultured cell trees, there is a strong linear correlation between the accumulation of slippage mutations and the number of cell divisions (10). Our group also recently obtained *in vivo* data that further supports this correlation. In mice with the same genetic background as the mice described here, it was found that the depth of mitotically active B lymphocytes increased linearly with the age of the animals, whereas the depth of satellite stem cells (which undergo very few or no mitoses in adult life) remained relatively constant (14). In the present study, cancer cells had an average depth of 236 cell divisions, which corresponds to $\sim$0.86 cell divisions per day. Although normal T lymphocytes were not extracted and therefore a direct comparison could not be made, our group recently found that in mice with the same genetic background, normal B lymphocytes divide at a rate of aproximately one division per day (14). It has previously been suggested that cancerous transformation may result in a shorter cell cycle (34) and, therefore, in a larger number of cell divisions. However, it is important to note that growth of a tumor cell population does not necessitate shortening of the cell cycle, and longer-than-normal cell cycles have been documented in cancer cells (35). Indeed, the fact that in the present study, tumor cells divided at a rate that is slightly smaller than the rate that was observed for normal B-lymphocytes in mice with the same genetic background strengthens the possibility that the cell cycle in tumor cells was not shortened. The average depth of tumor cells was almost twice the depth of cells from adjacent normal lung epithelium. This large and significant difference in depths most likely represents underlying differences in physiologic cell turnover rates between normal lymphocytes and lung epithelial cells. The striking difference in cell depths that were measured for cells that were separated by several micrometers in the same tissue section (on the two sides of the tumor-lung epithelium interface) attests to the precision and discriminating power of the method.

Mutation in *TP53*. The specific *TP53* mutation that was found here in some cancer cells was previously shown to be associated with skin tumors caused by UV irradiation and was proposed to result from direct damage to DNA from UV light, through a mechanism involving dimerization of cytosines (32). However, the mutation described here could not have been caused by UV light because the tumor was internal, and the animal was not exposed to UV light. The mutation was also not likely caused directly by MLH1 deficiency because, in contrast to slippage mutations in repeated sequences, point mutations have not been shown to occur at accelerated rates in MLH1 $-/-$ mice. Whether generated by a random somatic event or via an indirect effect of MLH1 $-/-$ deficiency, the mutation may have provided a growth or selection advantage to the developing clone and, thus, contributed to development of the cancer. The *TP53* mutation is not likely to have caused elevated MS mutation rates because mutations in P53 have been shown to be unassociated with MS instability in a variety of human cancers such as prostate (33), gastric (34), and esophageal (35) carcinomas. In human colorectal cancer, mutations in P53 have been shown to be inversely correlated with MS instability (36–38). However, this negative correlation is not likely to be due to decreased MS mutation rates in tumors with P53 mutations but, rather, is likely to reflect the fact that in colorectal cancer, mutations in *TP53* and in *MMR* genes represent two independent pathways to cancer pathogenesis (i.e., the "chromosomal instability" versus the "microsatellite instability" pathways; ref. 39).

Future applications. The ability to obtain data regarding the physical appearance, precise anatomic position, genotypic profile, and lineage position of single cells in a tumor may prove to be a powerful new tool for cancer research. It could readily be used in experimental animals to investigate basic aspects of cancer pathogenesis such as timing of tumor initiation, progression from premalignant to malignant states, physical growth patterns of tumors, clonal evolution within cancer cell populations, timing of metastasis formation, and the mechanisms underlying differential response to therapy. Furthermore, the fact that the procedure uses retrospective analysis means that it could also be used to investigate human tumors that are surgically removed from cancer patients (see Supplementary Text S5).

Although extensive work has been carried out on the molecular mechanisms underlying the cancer phenotype, the approach presented here can address the underlying demographic process of cancer development. We intend to apply this method to study key questions in human cancers, including at what stage does metastasis occur? Can the depth of tumor cells serve as a prognostic marker for cancer severity? Does chemotherapy target a subset of cells characterized by distinct lineage features (e.g., greater depth)? We believe single cell lineage studies of cancer cells can greatly enhance our understanding of cancer progression.

Disclosure of Potential Conflicts of Interest

No potential conflicts of interest were disclosed.

Acknowledgments

Received 11/12/2007; revised 3/19/2008; accepted 4/29/2008.

Grant support: Kahn Family Foundation, The Israel Academy of Science and Humanities (Bikura), The Yeshaya Horowitz association through the center for Complexity Science, The Research Grant from Dr. Mordecai Roshwald, The Grant from Kenneth and Sally Leafman Appelbaum Discovery Fund, The Estate of Karl Felix Jakubskind, The Clore Center for Biological Physics, and Flight Attendants Medical Research Institute.

The costs of publication of this article were defrayed in part by the payment of page charges. This article must therefore be hereby marked *advertisement* in accordance with 18 U.1S.C. Section 1734 solely to indicate this fact.

References

1. Bernards R, Weinberg RA. A progression puzzle. Nature 2002;418:823.
2. Shibata D, Navidi W, Salovaara R, Li ZH, Aaltonen LA. Somatic microsatellite mutations as molecular tumor clocks. Nat Med 1996;2:676–81.
3. Tsao JL, Zhang J, Salovaara R, et al. Tracing cell fates in human colorectal tumors from somatic microsatellite mutations: evidence of adenomas with stem cell architecture. Am J Pathol 1998;153:1189–200.
4. Tsao JL, Tavare S, Salovaara R, et al. Colorectal adenoma and cancer divergence. Evidence of multilineage progression. Am J Pathol 1999;154:1815–24.
5. Tsao JL, Yatabe Y, Salovaara R, et al. Genetic reconstruction of individual colorectal tumor histories. Proc Natl Acad Sci U S A 2000;97:1236–41.
6. Calabrese P, Tavare S, Shibata D. Pretumor progression: clonal evolution of human stem cell populations. Am J Pathol 2004;164:1337–46.
7. Morandi L, Pession A, Marucci GL, et al. Intraepidermal cells of Paget's carcinoma of the breast can be genetically different from those of the underlying carcinoma. Hum Pathol 2003;34:1321–30.
8. Maley CC, Galipeau PC, Li X, et al. The combination of genetic instability and clonal expansion predicts progression to esophageal adenocarcinoma. Cancer Res 2004;64:7629–33.
9. Maley CC, Galipeau PC, Finley JC, et al. Genetic clonal diversity predicts progression to esophageal adenocarcinoma. Nat Genet 2006;38:468–73.
10. Frumkin D, Wasserstrom A, Kaplan S, Feige U, Shapiro E. Genomic variability within an organism exposes its cell lineage tree. PLoS Comput Biol 2005;1:e50.
11. Wasserstrom A, Adar R, Shefer G, et al. Reconstruction of cell lineage trees in mice. PloS ONE 2008;3:e1939.
12. Salipante SJ, Horwitz MS. Phylogenetic fate mapping. Proc Natl Acad Sci U S A 2006;103:5448–53.
13. Salipante SJ, Horwitz MS. A phylogenetic approach to mapping cell fate. Curr Top Dev Biol 2007;79:157–84.
14. Wasserstrom A, Frumkin D, Adar R, et al. Estimating cell depth from somatic mutations. PLoS Comput Biol 2008;4:e1000058.
15. Frumkin D, Wasserstrom A, Itzkovitz S, et al. Amplification of multiple genomic loci from single cells isolated by laser micro-dissection of tissues. BMC Biotechnol 2008;8:17.
16. Nowell PC. The clonal evolution of tumor cell populations. Science 1976;194:23–8.
17. Fidler IJ, Kripke ML. Metastasis results from preexisting variant cells within a malignant tumor. Science 1977;197:893–5.
18. Breivik J. The evolutionary origin of genetic instability in cancer development. Semin Cancer Biol 2005;15:51–60.
19. Merlo LM, Pepper JW, Reid BJ, Maley CC. Cancer as an evolutionary and ecological process. Nat Rev Cancer 2006;6:924–35.
20. Jones TD, Wang M, Eble JN, et al. Molecular evidence supporting field effect in urothelial carcinogenesis. Clin Cancer Res 2005;11:6512–9.
21. Shattuck TM, Westra WH, Ladenson PW, Arnold A. Independent clonal origins of distinct tumor foci in multifocal papillary thyroid carcinoma. N Engl J Med 2005;352:2406–12.
22. Asplund A, Sivertsson A, Backvall H, et al. Genetic mosaicism in basal cell carcinoma. Exp Dermatol 2005;14:593–600.
23. Thliveris AT, Halberg RB, Clipson L, et al. Polyclonality of familial murine adenomas: analyses of mouse chimeras with low tumor multiplicity suggest short-range interactions. Proc Natl Acad Sci U S A 2005;102:6960–5.
24. Ramaswamy S, Ross KN, Lander ES, Golub TR. A molecular signature of metastasis in primary solid tumors. Nat Genet 2003;33:49–54.
25. Weigelt B, van't Veer LJ. Hard-wired genotype in metastatic breast cancer. Cell Cycle 2004;3:756–7.
26. Baker SM, Plug AW, Prolla TA, et al. Involvement of mouse Mlh1 in DNA mismatch repair and meiotic crossing over. Nat Genet 1996;13:336–42.
27. Aharoni R, Arnon R, Eilam R. Neurogenesis and neuroprotection induced by peripheral immunomodulatory treatment of experimental autoimmune encephalomyelitis. J Neurosci 2005;25:8217–28.
28. Prolla TA, Baker SM, Harris AC, et al. Tumour susceptibility and spontaneous mutation in mice deficient in Mlh1, Pms1 and Pms2 DNA mismatch repair. Nat Genet 1998;18:276–9.
29. Ellegren H. Microsatellites: simple sequences with complex evolution. Nat Rev Genet 2004;5:435–45.
30. Saitou N, Nei M. The neighbor-joining method: a new method for reconstructing phylogenetic trees. Mol Biol Evol 1987;4:406–25.
31. Efeyan A, Serrano M. p53: guardian of the genome and policeman of the oncogenes. Cell Cycle 2007;6:1006–10.
32. You YH, Szabo PE, Pfeifer GP. Cyclobutane pyrimidine dimers form preferentially at the major p53 mutational hotspot in UVB-induced mouse skin tumors. Carcinogenesis 2000;21:2113–7.
33. Mathis L, Nicolas JF. Cellular patterning of the vertebrate embryo. Trends Genet 2002;18:627–35.
34. Cemerikic-Martinovic V, Trpinac D, Ercegovac M. Correlations between mitotic and apoptotic indices, number of interphase NORs, and histological grading in squamous cell lung cancer. Microsc Res Tech 1998;40:408–17.
35. Boll IT. Documentation of normal and leukemic myelopoietic progenitor cells with high-resolution phase-contrast time-lapse cinematography. Onkologie 2001;24:395–402.
36. Shen L, Toyota M, Kondo Y, et al. Integrated genetic and epigenetic analysis identifies three different subclasses of colon cancer. Proc Natl Acad Sci U S A 2007;104:18654–9.
37. Chang SC, Lin JK, Yang SH, et al. Relationship between genetic alterations and prognosis in sporadic colorectal cancer. Int J Cancer 2006;118:1721–7.
38. Kim GP, Colangelo LH, Wieand HS, et al. Prognostic and predictive roles of high-degree microsatellite instability in colon cancer: a National Cancer Institute-National Surgical Adjuvant Breast and Bowel Project Collaborative Study. J Clin Oncol 2007;25:767–72.
39. Soreide K, Janssen EA, Soiland H, Korner H, Baak JP. Microsatellite instability in colorectal cancer. Br J Surg 2006;93:395–406.

Cell Lineage Analysis of a Mouse Tumor

Dan Frumkin, Adam Wasserstrom, Shalev Itzkovitz, et al.

Cancer Res 2008;68:5924-5931.